

HOSTED BY



ELSEVIER

Contents lists available at ScienceDirect

China University of Geosciences (Beijing)

Geoscience Frontiers

journal homepage: www.elsevier.com/locate/gsf

Research paper

Metasomatic origin of garnet xenocrysts from the V. Grib kimberlite pipe, Arkhangelsk region, NW Russia

E.V. Shchukina*, A.M. Agashev, N.P. Pokhilenko

Sobolev Institute of Geology and Mineralogy, Siberian Branch Russian Academy of Sciences, Koptyuga Pr. 3, Novosibirsk 630090, Russia

ARTICLE INFO

Article history:

Received 5 February 2016

Received in revised form

4 August 2016

Accepted 18 August 2016

Available online xxx

Keywords:

Lithospheric mantle

Mantle xenolith

Lherzolite-harzburgite-wehrlite-megacryst

paragenesis

Trace element

Major element

Kimberlite

ABSTRACT

This paper presents new major and trace element data from 150 garnet xenocrysts from the V. Grib kimberlite pipe located in the central part of the Arkhangelsk diamondiferous province (ADP). Based on the concentrations of Cr₂O₃, CaO, TiO₂ and rare earth elements (REE) the garnets were divided into seven groups: (1) lherzolitic “depleted” garnets (“Lz 1”), (2) lherzolitic garnets with normal REE patterns (“Lz 2”), (3) lherzolitic garnets with weakly sinusoidal REE patterns (“Lz 3”), (4) lherzolitic garnets with strongly sinusoidal REE patterns (“Lz 4”), (5) harzburgitic garnets with sinusoidal REE patterns (“Hz”), (6) wehrlitic garnets with weakly sinusoidal REE patterns (“W”), (7) garnets of megacryst paragenesis with normal REE patterns (“Meg”). Detailed mineralogical and geochemical garnet studies and modeling results suggest several stages of mantle metasomatism influenced by carbonatite and silicate melts. Carbonatitic metasomatism at the first stage resulted in refertilization of the lithospheric mantle, which is evidenced by a nearly vertical CaO-Cr₂O₃ trend from harzburgitic (“Hz”) to lherzolitic (“Lz 4”) garnet composition. Harzburgitic garnets (“Hz”) have probably been formed by interactions between carbonatite melts and exsolved garnets in high-degree melt extraction residues. At the second stage of metasomatism, garnets with weakly sinusoidal REE patterns (“Lz 3”, “W”) were affected by a silicate melt possessing a REE composition similar to that of ADP alkaline mica-poor picrites. At the last stage, the garnets interacted with basaltic melts, which resulted in the decrease CaO-Cr₂O₃ trend of “Lz 2” garnet composition. Cr-poor garnets of megacryst paragenesis (“Meg”) could crystallize directly from the silicate melt which has a REE composition close to that of ADP alkaline mica-poor picrites. *P-T* estimates of the garnet xenocrysts indicate that the interval of ~60–110 km of the lithospheric mantle beneath the V. Grib pipe was predominantly affected by the silicate melts, whereas the lithospheric mantle deeper than 150 km was influenced by the carbonatite melts.

© 2016, China University of Geosciences (Beijing) and Peking University. Production and hosting by Elsevier B.V. This is an open access article under the CC BY-NC-ND license (<http://creativecommons.org/licenses/by-nc-nd/4.0/>).

1. Introduction

Mantle samples (xenoliths, xenocrysts, megacrysts) brought to the surface by kimberlites provide information about the composition and the evolution of the continental upper mantle. The lithospheric mantle beneath Archean cratons is composed predominantly by peridotites and less common eclogites and pyroxenites. It is generally accepted that lithospheric mantle peridotites are residues of extensive partial melting (harzburgites and perhaps

dunites, e.g. Sobolev et al., 1969, 1977; Efimova and Sobolev, 1977; Stachel et al., 1998; Griffin et al., 2003; Agashev et al., 2013; Doucet et al., 2013). Clinopyroxenes and garnets are regarded as later metasomatic products in ultra-depleted peridotites (e.g. Simon et al., 2007; Agashev et al., 2013; Pokhilenko et al., 2015), though some garnets can survive partial melting (Doucet et al., 2013; Shchukina et al., 2015). Ubiquitous evidence for mantle metasomatism is found in mantle samples of different cratons worldwide (e.g. Menzies et al., 1987; Pokhilenko et al., 1993). Features of metasomatic enrichment of mantle samples are recorded in (i) modal mineralogy, i.e. presence of phlogopite and amphibole in xenoliths (e.g. Carswell, 1973; Harte, 1983; Erlank et al., 1987; Menzies and Hawkesworth, 1987; Achterbergh et al., 2001; Gregoire et al., 2003; Simon et al., 2003; Bell et al., 2005; Solovyeva et al., 2012), (ii) trace element composition of garnet

* Corresponding author.

E-mail addresses: helenashchukina@gmail.com, shukinalena@igm.nsc.ru (E.V. Shchukina).

Peer-review under responsibility of China University of Geosciences (Beijing).

<http://dx.doi.org/10.1016/j.gsf.2016.08.005>1674-9871/© 2016, China University of Geosciences (Beijing) and Peking University. Production and hosting by Elsevier B.V. This is an open access article under the CC BY-NC-ND license (<http://creativecommons.org/licenses/by-nc-nd/4.0/>).

and clinopyroxene (e.g. Hoal et al., 1994; Griffin et al., 1999; Simon et al., 2003; Burgess and Harte, 2004; Agashev et al., 2013; Howarth et al., 2014), (iii) difference between measured and calculated bulk rock compositions (e.g. Sobolev et al., 1999a,b; Agashev et al., 2013), and (iv) incompatible element ratio (e.g. Agashev et al., 2013). Major and trace element compositions of mantle-derived garnets show melting and metasomatic history of their host rocks and provide useful insights into the evolution of the lithospheric mantle beneath Archean cratons (Shimizu and Richardson, 1987; Hoal et al., 1994; Shimizu et al., 1997a,b; Stachel et al., 1998, 2004; Griffin et al., 1999; Gregoire et al., 2003; Burgess and Harte, 2004; Simon et al., 2007; Gibson et al., 2008; Agashev et al., 2013; Doucet et al., 2013; Ziberna et al., 2013; Howarth et al., 2014). High-chromium garnets with sinusoidal REE patterns, i.e. harzburgitic and dunitic varieties (Sobolev et al., 1973) belonging to G10 garnets according to the classification of Dawson and Stephens (1975) and Gurney (1984) are indicative for diamond potential in kimberlites.

The lithospheric mantle beneath the Arkhangelsk diamondiferous province (ADP) is one of the most poorly characterized mantle sections beneath kimberlite occurrences worldwide. There are relatively few studies on the composition and thermal state of the lithospheric mantle of ADP and trace element variations in mantle minerals (Sablukov et al., 2000; Kostrovitsky et al., 2004; Lehtonen et al., 2009; Shchukina et al., 2012, 2015; Afanasiev et al., 2013). Considerable information about the structure and composition of lithospheric mantle beneath ADP was obtained through the study of mineral inclusions in diamonds from the Lomonosovo (Sobolev et al., 1997a,b, 2009a,b) and Grib (Malkovets et al., 2011) deposits. The finding of garnets with majorite component and omphacite with high K₂O contents (up to 0.8 wt.%) among inclusions in diamonds evidences for higher pressure conditions of ADP diamond formation compared to the majority of diamond deposits worldwide (Sobolev et al., 1997a,b, 2009a,b). Metasomatic evolution of the lithospheric mantle beneath the V. Grib pipe, based on the detailed study of peridotite samples, has been previously discussed (Shchukina et al., 2015). Herein, we present major and trace element data for garnet xenocrysts of the late Devonian V. Grib kimberlite pipe. These xenocrysts were selected for better characterization of the composition and metasomatic evolution of the lithospheric mantle beneath the central part of ADP.

2. Geological setting and samples

The Arkhangelsk diamondiferous province (ADP) is located in the northern part of the East European Platform and includes several magmatic fields (Fig. 1): the Zolotitsa kimberlite field; the Kepino and the Verhotina fields of kimberlites and olivine melilitites; the Turiyno basaltic field; the Izhmzero field of olivine melilitite and picrite; and the Mela field of kimberlite and carbonate (Sobolev et al., 1992; Bogatikov et al., 1999; Mahotkin et al., 2000; Garanin, 2004). ADP hosts two large diamond deposits: the Lomonosovo deposit of the Zolotitsa field with five kimberlite pipes (Arkhangelskaya, Lomonosovskaya, Pionerskaya, Karpinskaya-1, Karpinskaya-2) and the V. Grib kimberlite pipe deposit. Kimberlites from both deposits contain abundant mantle xenoliths (Sablukov et al., 2000; Kostrovitsky et al., 2004; Lehtonen et al., 2009; Shchukina et al., 2012, 2015), but those from the Lomonosovo deposit are extremely altered compared to those of the V. Grib pipe. The V. Grib pipe is located in the Verhotina field in the central part of ADP (Bogatikov et al., 1999). According to Rb-Sr age dating of kimberlites, the age of the V. Grib kimberlite pipe is 372 ± 8 Ma (Shevchenko et al., 2004). The pipe intrudes Vendian sedimentary rocks and is covered by terrigenous-carbonate rocks of middle

Carboniferous and unconsolidated Quaternary sediments, with a total thickness of about 70 m. There are crater and diatreme parts in the structure of the V. Grib pipe. The crater facies consists of various volcanoclastic, volcanoclastic-sedimentary and sedimentary rocks with abundant xenoliths of terrigenous host rocks (Bogatikov et al., 1999). The diatreme consists of tuff breccias, xeno-tuff breccias and kimberlites.

150 garnet grains with sizes ranging between 0.5 and 1 mm were randomly selected for the present study from heavy mineral concentrate of the V. Grib kimberlite. Grain colors vary from reddish orange and red to purple and violet. Garnets are presented by single grains without inclusions of any mineral phases.

3. Methods

The major element composition of garnet was determined by electron probe microanalysis (EPMA) in the Analytical Center for multi-element and isotope research SB RAS (Novosibirsk, Russia) using a JEOL JXA-8100 microanalyzer. The analyses were performed with an accelerating voltage of 20 kV and a 50 nA beam current, with a counting time of 10 s for peaks and 5 s for background (Lavrent'ev et al., 2015). The relative standard deviation did not exceed 1.5%. Ni concentrations were performed with an accelerating voltage of 25 kV and a 300 nA beam current the counting time of 400 s for peaks and background (Lavrent'ev et al., 2006). Trace elements in garnet were analyzed in the Analytical Center for multi-element and isotope research SB RAS (Novosibirsk, Russia)

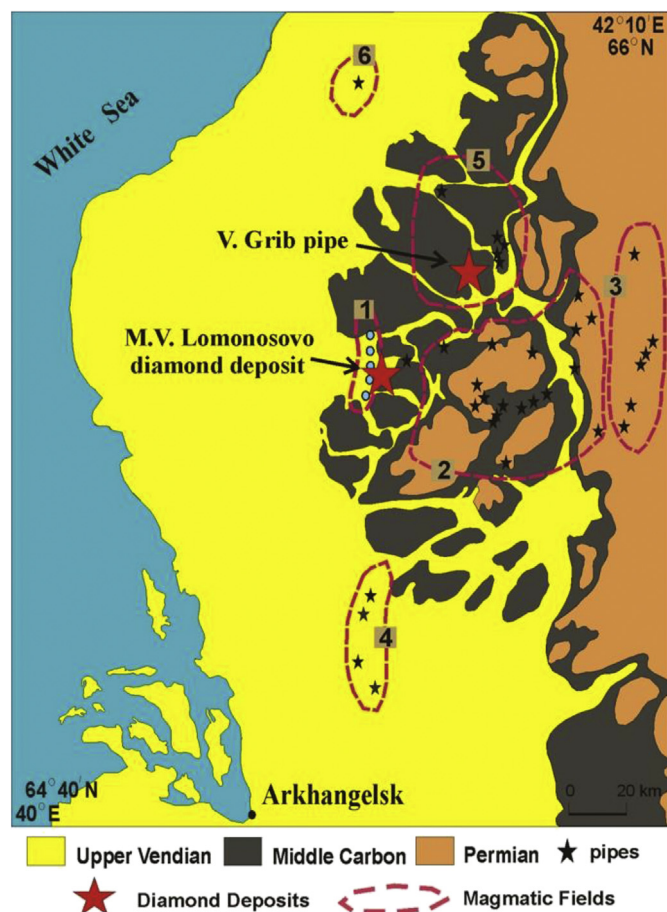


Figure 1. Simplified geological map of the Arkhangelsk diamondiferous province. 1 – Zolotitsa field, 2 – Kepino field, 3 – Turiyno field, 4 – Izhmzero field, 5 – Verhotina field, 6 – Mela field.

using Finnigan Mat Element Inductively coupled plasma mass spectrometry (ICPMS) equipped with Nd:YAG nm 266 LaserProbe system. The laser was operated at 20 Hz with a 12 mJ cm^{-2} pulse energy and beam size of $80 \mu\text{m}$. Helium was used as a carrier gas. The acquisition time was 90 s for background and 60 s for a signal. The reference samples SRM NIST 612, NIST 614 were used as external standards. The concentrations of Ca determined by EPMA were used as internal standards to overcome the matrix effect.

4. Analytical results

4.1. Major and trace element composition

EPMA and trace element data of the garnet xenocrysts are provided in the [Supplementary file 1](#). All garnet xenocrysts were divided into the following groups according to Cr_2O_3 , CaO and TiO_2 concentrations (Sobolev et al., 1973): 68% of garnets (102 grains) plot the field of lherzolite paragenesis; 14% (21 grains) – megacryst paragenesis; 11% (17 grains) – eclogite paragenesis; 6% (9 grains) – harzburgite paragenesis; 1% (1 grain) – wehrlite paragenesis (Fig. 2). This study is focused on peridotitic garnets. Chondrite-normalized REE patterns for peridotitic garnets are shown in Fig. 3.

Lherzolitic garnets can be divided into four groups according to the shape of their chondrite-normalized REE patterns and using the division by Shchukina et al. (2015) initially applied for garnets in peridotite xenoliths of the V.Grib pipe (Shchukina et al., 2015): (1) “depleted” garnets, (2) garnets with flat REE patterns, (3) garnets with weakly sinusoidal REE patterns, (4) garnets with sinusoidal REE patterns (Fig. 3). One garnet from the 1-st group (1 grain G65, “Lz 1”) is characterized by moderate concentrations of CaO (2.4 wt.%) and Cr_2O_3 (4.4 wt.%) with MREE at C1 chondrite unit (McDonough and Sun, 1995), $(\text{Sm}/\text{Er})_n = 0.03$, $(\text{La}/\text{Yb})_n = 0.002$. This garnet has gradually increased ranging from La to Yb and contains low Y (12 ppm), Zr (0.8 ppm), Ti (400 ppm) concentrations. In the Y/Zr diagram, the garnet from the first group matches the field of “depleted” garnets from the V. Grib peridotites (Fig. 4).

Garnets from the second group (51 grains, “Lz 2”) are characterized by moderate concentrations of Cr_2O_3 (0.45–6.0 wt.%) and CaO (3.5–5.9 wt.%), MREE at 2–13 chondrite units, $(\text{Sm}/\text{Er})_n < 1$ (0.16–0.98), $(\text{La}/\text{Yb})_n = (0.001–0.060)$ and have flat patterns from MREE to HREE (Fig. 3). Two garnet grains (G42, G67) are enriched in LREE with $(\text{La}/\text{Yb})_n = (0.9–0.111)$. The G67 garnet is extremely depleted in MREE. There is a positive correlation of Y and Zr contents in “Lz 2” garnets (Fig. 4).

Garnets from the third group (28 grains, “Lz 3”) show significant variability of Cr_2O_3 values (1.0–9.2 wt.%), contain MREE at 5–14 chondrite units with $(\text{Sm}/\text{Er})_n > 1$ (1.05–4.81) and $(\text{La}/\text{Yb})_n = (0.010–0.051)$. “Lz 3” garnets have a gradually increasing range from LREE to MREE with the peak in MREE and slightly decreasing range from MREE to HREE (Fig. 3). Two samples are different from the total group: the G85 sample is enriched in LREE with $(\text{La}/\text{Yb})_n = 0.607$; the G68 sample is depleted in MREE. “Lz 3” garnets have less Y content (3–14 ppm) compared to garnets “Lz 2”. The Zr content in “Lz 3” garnets ranges from 6 to 58 ppm.

Garnets from the fourth group (21 grains, “Lz 4”) contain high Cr_2O_3 (4.9–11.3 wt.%) and moderate CaO (4.4–6.2 wt.%). This group has a sinusoidal REE pattern with $(\text{Sm}/\text{Er})_n > 4$ (4.2–27.2) and $(\text{La}/\text{Yb})_n = (0.020–1.546)$. Y/Zr ratios are similar to garnets of harzburgite paragenesis.

The average Cr_2O_3 content and $\text{Mg}^\#$ increase in the following sequence: “Lz 1” ($\text{Cr}_2\text{O}_3 = 2.4 \text{ wt.}\%$; $\text{Mg}^\# = 73$) < “Lz 2” ($\text{Cr}_2\text{O}_3 = 3.3 \text{ wt.}\%$; $\text{Mg}^\# = 76$) < “Lz 3” ($\text{Cr}_2\text{O}_3 = 5.7 \text{ wt.}\%$; $\text{Mg}^\# = 78$) < “Lz 4” ($\text{Cr}_2\text{O}_3 = 7.9 \text{ wt.}\%$; $\text{Mg}^\# = 79$) (Fig. 5). The average Y/Zr ratio decreases in the following sequence: “Lz 1” (14.9) > “Lz 2” (0.6) > “Lz 3” (0.2) > “Lz 4” (0.08).

Garnets of megacryst paragenesis (21 grains, “Meg”) contain moderate concentrations of Cr_2O_3 (2.2–3.4 wt.%) and CaO (4.4–5.4 wt.%), and a high TiO_2 content (0.9–1.3 wt.%) with average $\text{Mg}^\# = 0.75$. These garnets have flat REE patterns with $(\text{Sm}/\text{Er})_n < 1$ (0.2–0.6), and $(\text{La}/\text{Yb})_n = (0.001–0.012)$ (Fig. 3). The Y/Zr ratios are similar to “Lz 2” garnets. These garnets have higher average REE concentrations of high field strength elements (HFSE) group than garnet megacrysts described previously (Kostrovitsky et al., 2004). There is a strong correlation of TiO_2 with Zr contents in “Meg” garnets and excellent correlation between Zr and Hf, Zr and Er (and other HREE).

Garnets of harzburgite paragenesis (9 grains, “Hz”) contain high Cr_2O_3 (7.9–10.4 wt.%) and moderate CaO (2.6–5.3 wt.%) concentrations with average $\text{Mg}^\# = 0.8$. These garnets have sinusoidal REE patterns with $(\text{Sm}/\text{Er})_n > 5$ (5.2–19.8), $(\text{La}/\text{Yb})_n = (0.04–1.4)$. The Y/Zr ratios are similar to “Lz 4” garnets.

A garnet of wehrlite paragenesis (one G45 grain, “W”) has high CaO (6.4 wt.%) and Cr_2O_3 (6.2 wt.%) contents, a weakly sinusoidal REE pattern with $(\text{Sm}/\text{Er})_n > 1$ (1.8) and $(\text{La}/\text{Yb})_n = 0.012$. This garnet contains low concentrations of Y (2 ppm), Zr (7 ppm), Ti

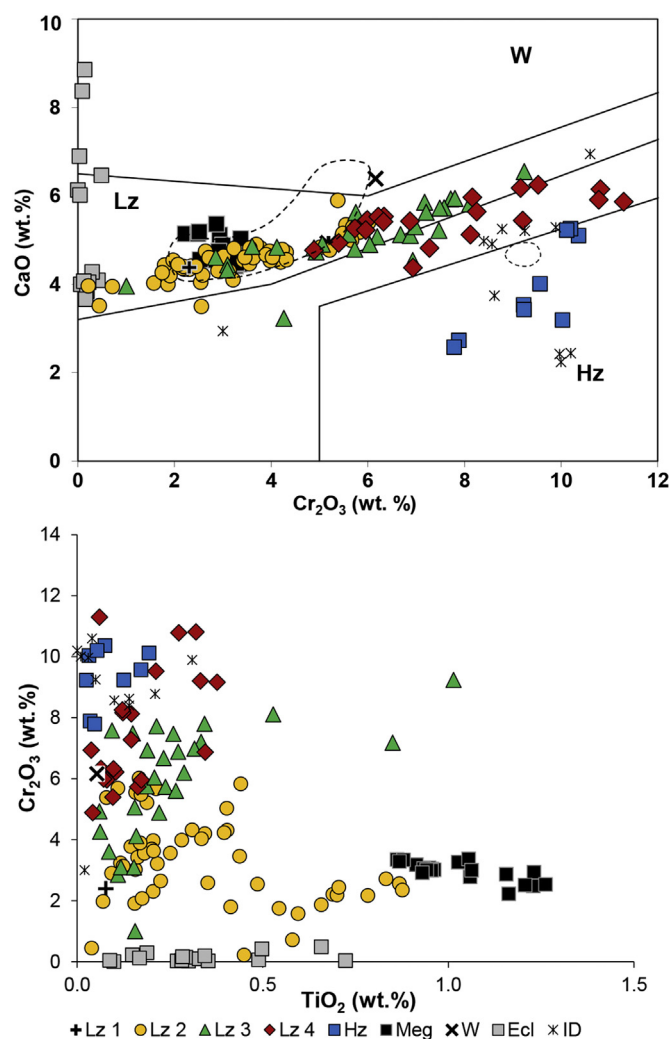


Figure 2. CaO- Cr_2O_3 and $\text{TiO}_2/\text{Cr}_2\text{O}_3$ variations in garnet xenocrysts from the V.Grib kimberlite pipe. Harzburgite (Hz), lherzolite (Lz), wehrlite (W) fields after Sobolev et al. (1973). Dotted line – compositions of garnets from the V. Grib peridotites (Shchukina et al., 2012, 2015). Lz – lherzolite paragenesis, Hz – harzburgite paragenesis, W – wehrlite paragenesis, Meg – megacryst paragenesis, Ecl – eclogite paragenesis, ID – inclusions in diamonds from the Lomonosovo field (Sobolev et al., 1997a,b, 2009a,b).

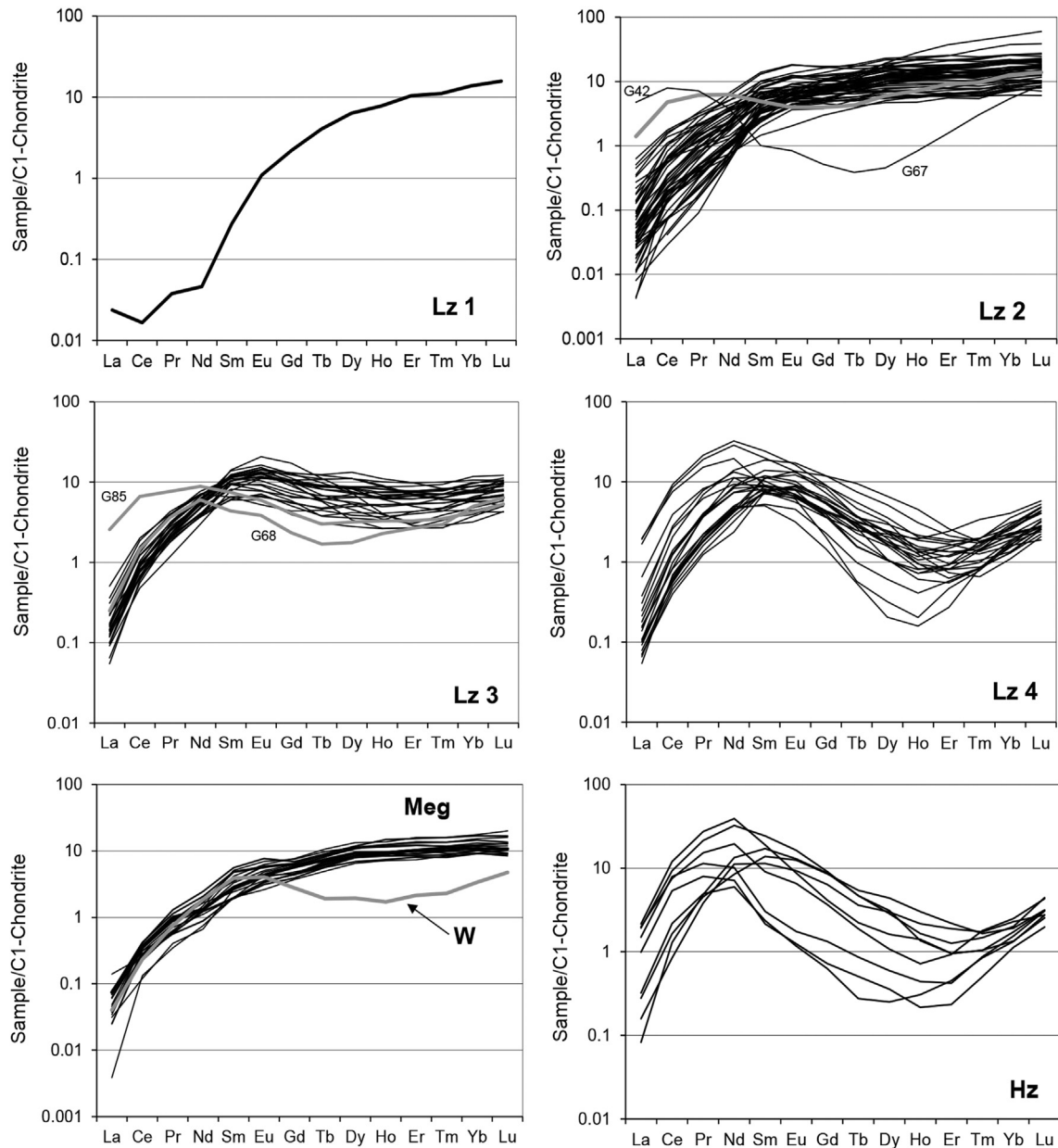


Figure 3. C1-Chondrite normalized (McDonough and Sun, 1995) REE profiles of V. Grib garnet xenocrysts.

(309 ppm). The Y/Zr ratio is similar to “Lz 3”, “Lz 4” and “Hz” garnets. It should be noted that garnet compositions from two lherzolite samples of V. Grib kimberlite match the field of “wehrlitic” garnets (Shchukina et al., 2012, 2015).

As shown in Fig. 2 some “Lz 3”, “Lz 4” and “Hz” garnets are close in composition to garnet inclusions in diamonds from the Lomonosovo field of ADP (Sobolev et al., 1997a,b, 2009a,b).

5. Pressure-temperature (PT) estimates

A brand new single crystal thermobarometer for garnets (Ashchepkov et al., 2010, 2011, 2012) was used to evaluate the PT conditions for garnet xenocrysts. This thermobarometer is calibrated on the basis of orthopyroxene-garnet thermobarometry (MacGregor, 1974; Brey and Kohler, 1990) using a large database of EPMA analyses of xenolith minerals, and provides internally consistent PT estimates with other methods (Ashchepkov et al.,

2010, 2011, 2012; Afanasiev et al., 2013). Equilibration temperatures of garnets also were obtained by Ni-thermometry (Ryan et al., 1996). The P parameters were determined by projecting of T onto peridotite-derived geotherm for the V. Grib pipe (Shchukina et al., 2012, 2015). The results are shown on Fig. 6 and in Supplementary file 1.

According to the thermobarometer (Ashchepkov et al., 2010, 2011, 2012) the most pronounced PT trends appear from 40 to 53 kbar along the 37 mW/m² geotherm, and from 24 to 40 kbar along 40–45 mW/m² geotherms (Pollack and Chapman, 1977). The geotherm is reasonably linear to about 55 kbar. In the 55–65 kbar interval, PT estimates for garnets plot in the field between the 35 and 45 mW/m² geotherms (Fig. 6A). Obviously, “Lz 2” and “Lz 3” garnets occur through the section of the lithospheric mantle up to 52 kbar (“Lz 2”) and 69 kbar (“Lz 3”). “Lz 4” garnets with sinusoidal REE patterns predominantly occur in the deeper part of the lithospheric mantle (42–55 kbar) in the diamond stability field. PT

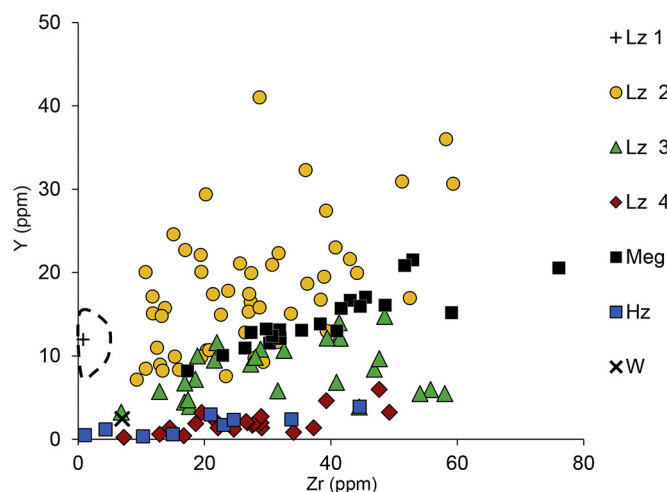


Figure 4. Y/Zr variations in garnet xenocrysts from the V. Grib kimberlite pipe. Dotted field – field of depleted garnet compositions from the V. Grib peridotites (Shchukina et al., 2015).

estimates of garnets “Hz” fall into two trends. The first one traces continuously the 35 mW/m² geotherm from 53 to 62 kbar. The second one is located in the 37–40 kbar interval between the 40 and 45 mW/m² geotherms. According to Ni-thermometry (Ryan et al., 1996) “Hz”, “Meg” and “Lz 4” garnets occur in intervals of lithospheric mantle between 42–55 kbar, whereas “Lz 2” and “Lz 3” garnets occur through all sections of the lithospheric mantle from 26 to 66 kbar (Fig. 6B). *PT* estimates for peridotite xenoliths (Shchukina et al., 2012, 2015) correspond to the 37 mW/m² conductive geotherm in the pressure interval from 20 to 75 kbar (Fig. 6C). *PT* profiles of garnet xenocrysts from the Arkhangelskaya pipe and the Carboniferous sandstone of ADP (Afanasiev et al., 2013), the Lesotho kimberlite (Nixon and Boyd, 1973a,b) and the Udachnaya pipe (Boyd et al., 1997; Agashev et al., 2013; Tychkov et al., 2014) provide evidence for heating of the lithospheric mantle base. However, no such heating event had been reported before for V. Grib peridotite xenoliths (Shchukina et al., 2012, 2015), megacrysts (Kostrovitsky et al., 2004) and xenocrysts (Afanasiev et al., 2013; this study).

6. Discussion

6.1. Origin of peridotitic garnets

6.1.1. Pre-metasomatic garnets

The following three types of garnets could be present in the early formed lithospheric mantle: low Cr₂O₃ (<4 wt.%) depleted residual garnets that survived partial melting (Shchukina et al., 2012, 2013, 2015), various chromium garnets that exsolved from high temperature Opx upon cooling (Dawson, 2004) and high-chromium garnets produced by the Opx + Sp – Grt + Ol reaction (MacGregor, 1964). Residual garnets have strongly positive sloped REE pattern with HREE contents of about 10 chondritic units and sharply increasing concentrations from La to Lu (Shchukina et al., 2015). Exsolved garnets have much more gentle sloped REE pattern with HREE content of 1–3 chondritic units and gradually increasing REE concentration in the same way as residual garnets. Garnets formed by Opx + Sp reaction probably have the similar REE pattern with exsolved garnets as they also inherited REE from Opx.

REE concentrations in V. Grib kimberlite peridotitic garnets indicate a metasomatic origin of all studied garnets except for the G65 (“Lz 1”) sample. This “Lz 1” garnet has no signs of metasomatic

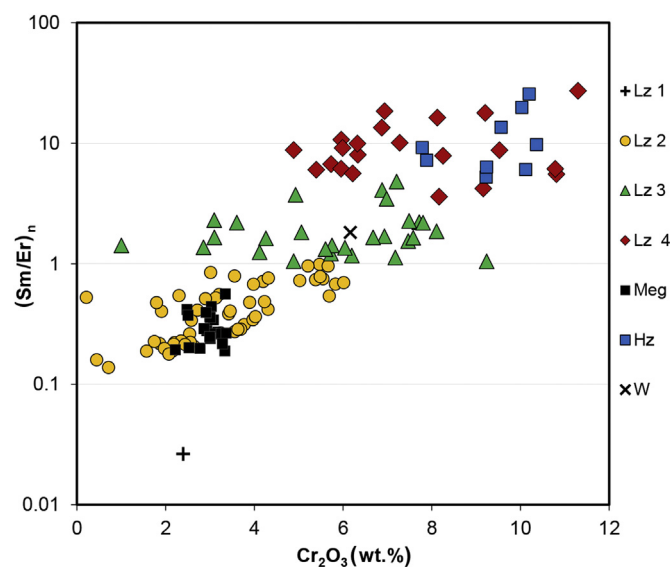


Figure 5. (Sm/Er)_n vs. Cr₂O₃ in garnet xenocrysts from the V. Grib kimberlite pipe.

origin. Low Y/Zr, (Sm/Er)_n and (La/Yb)_n ratios indicate its residual nature without any influence of metasomatic fluids. In the Y/Zr diagram, the G65 garnet plots in the field of residual garnets from V. Grib peridotites (Shchukina et al., 2015). It should be noted that the depleted garnet field from the V. Grib pipe is not identical to the depleted garnet field according to Griffin et al. (1999). Depleted garnets also were identified in six V. Grib lherzolite samples (Shchukina et al., 2015). Garnets from three lherzolite samples (Shchukina et al., 2015) are slightly enriched in LREE with weak negative Eu anomaly and clinopyroxenes are strongly enriched in LREE (80–280 chondrite unites) with a high (La/Yb)_n ratio, which is a result of carbonatite melt influence (Shchukina et al., 2015).

6.1.2. Metasomatic garnets

“Lz 2” and “Meg” garnets have normal REE patterns with positive slopes for LREE and nearly flat to positive slope for MREE and HREE, typical for garnets from fertile (or refertilized) lherzolites (e.g. Agashev et al., 2013; Howarth et al., 2014). There is a positive correlation between Y and Zr concentrations corresponding to the “melt” metasomatic trend according to the definition by Griffin et al. (1999). Generally, the garnets of this type occur together with clinopyroxenes in peridotites (Agashev et al., 2013; Howarth et al., 2014; Shchukina et al., 2015). “Lz 2” garnets are the most wide spread in the V. Grib peridotites (Shchukina et al., 2015). As it was shown by the recent results of geochemical modeling of fractional crystallization (Shchukina et al., 2015), the formation of “Lz 2” garnets was influenced by a silicate melt with geochemical features similar to the Turiyno basalts of ADP.

“Lz 3” and “W” garnets have weakly-sinusoidal REE patterns. This type of garnet has also been reported among the diamonds inclusions (Stachel et al., 1998, 2004) and lherzolite samples worldwide (e.g. Stachel et al., 1998; Gregoire et al., 2003), including V. Grib lherzolites (Shchukina et al., 2015). In the Y/Zr diagram (Fig. 4) these garnets reveal individual trends which differ from the trend for garnets with normal and sinusoidal REE patterns. The latter could be evidence for the existence of at least three garnet generations (“Lz 2” + “Meg”, “Lz 3” + “W”, “Lz 4” + “Hz”) within the rocks that were probably reacted with different metasomatic agents. Recently it was found that “Lz 3” garnets from V. Grib peridotites were in equilibrium with silicate melt with a composition close to the Izhmzero picrites of ADP (Shchukina et al., 2015). These garnets were also in major-element equilibrium with

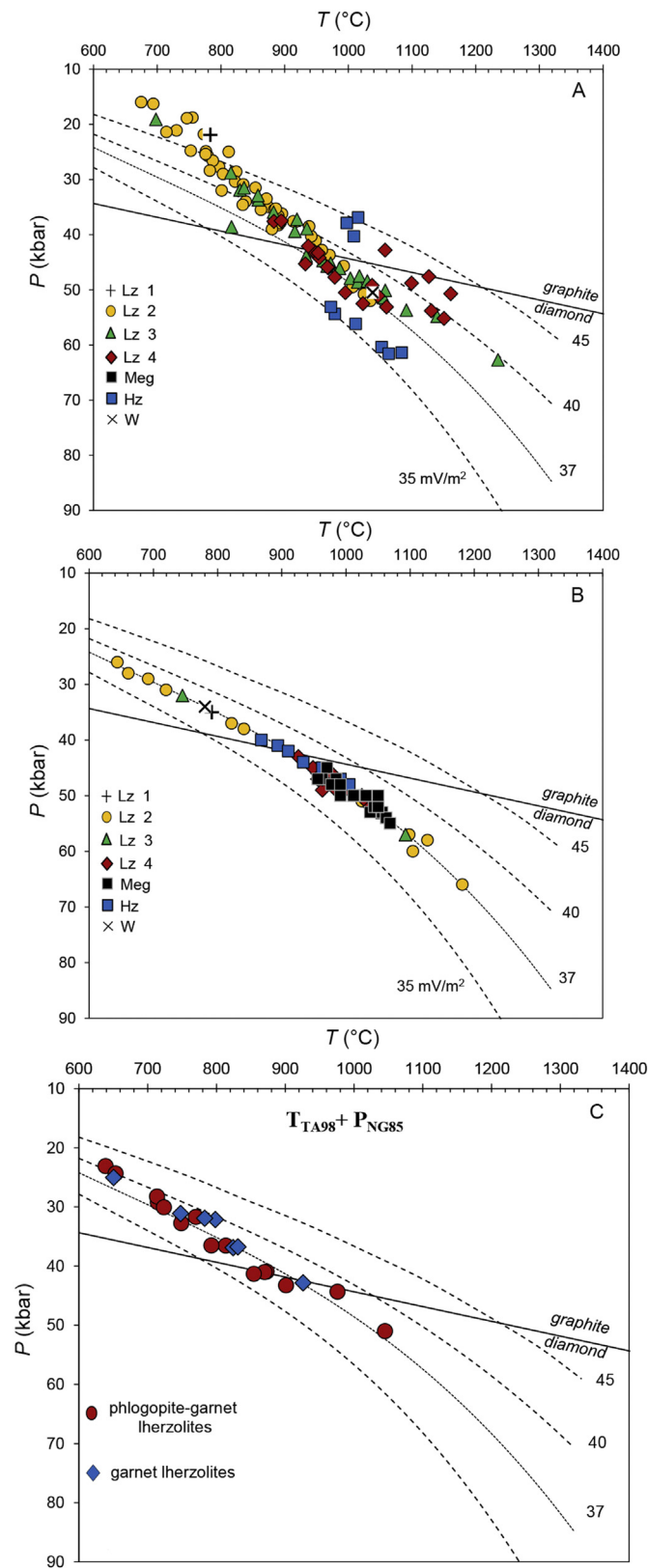


Figure 6. *P-T* estimates for V. Grib garnet xenocrysts (this study) and lherzolites (Shchukina et al., 2015). *P-T* parameters for garnet xenocrysts were calculated according to Ashchepkov et al. (2010, 2011, 2012) (A) and Ryan et al. (1996) (B). *P-T* parameters for garnet lherzolites (C) were calculated using the thermometer by Taylor (1998, T TA98) and barometer by Nickel and Green (1985, P NG85).

associated clinopyroxenes in V. Grib peridotite samples (Shchukina et al., 2015).

6.1.3. Origin of garnets with sinusoidal REE patterns

“Lz 4” and “Hz” garnets have sinusoidal REE patterns. The interpretation of sinusoidal REE patterns is still being discussed (e.g. Gibson et al., 2008). According to an experimental study (Canil and Wei, 1992), garnets with Cr₂O₃ contents above 4 wt.% cannot be a residual phase of peridotite melting. Theoretically, they can be formed by the Sp + Opx = Ol + Gar reaction (MacGregor, 1964) under the influence of carbonatite metasomatism (Agashev et al., 2013). Fig. 7 illustrates the average REE patterns in V. Grib “Lz 4” garnets and REE pattern in exsolved garnets from the Monastery pipe (Dawson, 2004) and the V. Grib pipe (unpublished data).

It is difficult to find terrestrial melts that could be in equilibrium with sinusoidal garnets. We approximated the REE composition of “Lz 4” garnets, suggesting the crystallization of a garnet with LREE and MREE corresponding to “Lz 4” garnets but with lower HREE (Fig. 7). The melt in equilibrium with approximated REE composition of the “Lz 4” garnet, which was calculated using the garnet/melt partition coefficients (Le Roex et al., 2003), is enriched in LREE (100–250 chondrite units) and extremely depleted in HREE (0.05–0.5 chondrite units) (Fig. 7). The model of formation of garnet with sinusoidal REE pattern from a fractionated melt was recently proposed (e.g. Ziberna et al., 2013; Shu and Brey, 2015). However, melt fractionation in the lithospheric mantle cannot reduce the concentration of Y and HREE in residual liquid at the time of garnet crystallization, as we show by fractional crystallization modeling in the next section. Therefore, we suggest that the sinusoidal REE pattern is produced by the reaction of exsolved garnets with melt/fluid that was not fractionated, but originally very poor in Y and HREE, and strongly enriched in incompatible elements (most probably carbonatitic in nature; Agashev et al., 2013; Pokhilenko et al., 2015; this study).

6.2. Geochemical modeling of fractional crystallization

6.2.1. Nature of metasomatic agents

Metasomatic agents operating in the lithospheric mantle are usually considered to be of two main types: silicate melts and carbonatite melts/fluids (Agashev et al., 2013; Pokhilenko et al., 2015). In many studies, authors make more detailed definitions of the metasomatic agents relating them to certain rock types, i.e. various basalts, kimberlites, lamproites and carbonatites (e.g. Hoal et al., 1994; Coltorti et al., 1999; Pokhilenko et al., 1999; Gregoire et al., 2003; Agashev et al., 2013; Doucet et al., 2013; Ziberna et al., 2013; Howarth et al., 2014). The definitions were usually made by calculation of liquid in equilibrium with garnets by simply dividing the garnet composition on the garnet/melt K_d and plotting the obtained composition on the PM/Chondrite normalized log-scale diagram. Many proposed melt compositions look very similar to each other on the log-scale diagram, being in reality very different in abundance of trace element.

Megacryst garnets are often regarded to be crystallized directly from the kimberlitic melt. However, for several reasons, we cannot agree with the latter opinion. Firstly, kimberlite is too low in Al₂O₃ (1–2 wt.%) to crystallize any significant amount of garnet. Secondly, according to modern data, initial kimberlitic melts are rather carbonatitic in composition (Agashev et al., 2001, 2008; Kamenetsky et al., 2009), and do not crystallize garnet, though can assimilate peridotitic minerals during ascent (Kamenetsky and Yaxley, 2015). Additionally kimberlite magmas are erupted in a short time span after their formation.

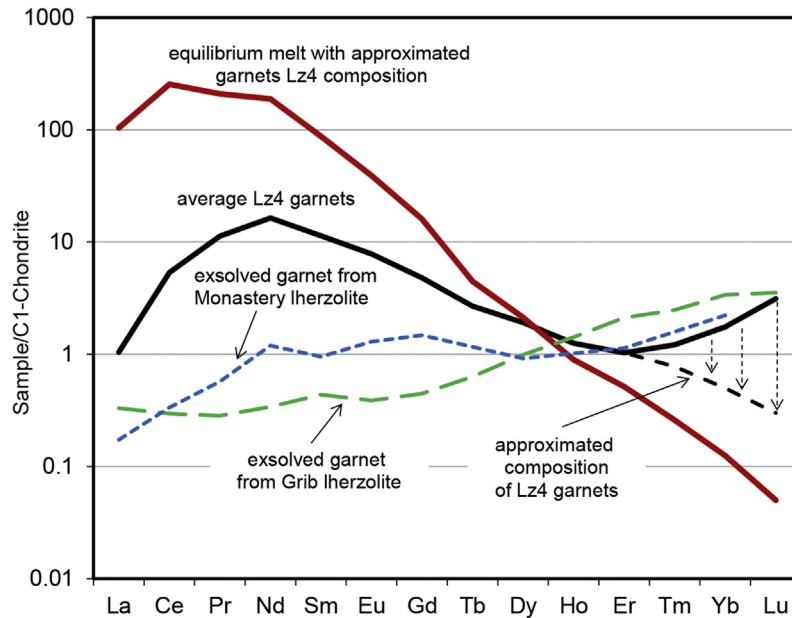


Figure 7. C1-Chondrite normalized (McDonough and Sun, 1995) REE patterns for hypothetical melt in equilibrium with the approximated “Lz 4” garnet composition.

To characterize the nature of the metasomatic agent, we used a new approach based on the covariation of trace elements assuming crystallization of megacryst garnets from the evolving magma.

6.2.2. Choosing the K_d and geochemical modeling

We have modeled the fractional crystallization of kimberlitic (Bogatikov et al., 1999), basaltic (Hauri, 1996) and picritic (Mahotkin et al., 2000) magmas with several K_d datasets (e.g. Hauri et al., 1994; Halliday et al., 1995; Green et al., 2000; Le Roex et al., 2003; Keshav et al., 2005; Tuff and Gibson, 2007) and different proportions of crystallized minerals. Most K_d datasets (Green et al., 2000; Keshav et al., 2005 see Fig. 8; Hauri et al., 1994; Halliday et al., 1995 not shown) don't work when crystallizing Gar and Cpx in 50/50% proportion as in this case, as garnets with negative correlation of Y and Zr are produced. The positive correlation of these elements (Fig. 8) is reproduced only with the basaltic K_d dataset of Tuff and Gibson (2007) and the kimberlitic dataset of Le Roex et al. (2003). To reproduce positive correlations, the bulk K_d of Y must be less than 1 (closer to 0.5), therefore the amount of garnet in the crystallized assemblage should not exceed 20%. As Grt and Cpx are more common megacrysts in kimberlites than Ol and Opx, the mineral/melt K_d for Y and HREE must be lower than that of most experimental data. The modeling results show that the typical magmatic trend of “Meg” garnets is similar to the composition of garnets crystallized from the ADP mica-poor picrites (Mahotkin et al., 2000), while “Lz 2” garnet compositions form a trend similar to the garnets crystallized from the basaltic melt (Hauri, 1996). In the Y/Zr diagram, “Lz 3” garnets show the intermediate position between “Lz 4” and “Meg” garnets (Fig. 4) and form two trends (Fig. 8): one similar to “Lz 4” garnets and another one to “Meg” garnets.

6.3. Geochemical evolution model

According to the obtained data, we can suggest that at least two general different types of metasomatic enrichment are evident in the chemical composition of garnet xenocrysts from the V. Grib kimberlite pipe: carbonatite and silicate metasomatic agents. A model of geochemical evolution of V. Grib garnet xenocrysts is graphically summarized in Fig. 9.

High Cr_2O_3 contents (7.8–10.4 wt.%) and low HREE contents (e.g. $\text{Yb} = 1.1\text{--}2.5 \times \text{Cl}$) of “Hz” garnets are consistent with the strongly depleted nature of pre-metasomatic protoliths. As proposed by Shchukina et al. (2015), the protolith of garnet dunite (G1-33 sample) which contains a high-chromium garnet of harzburgite paragenesis with sinusoidal REE patterns was formed after $\sim 50\%$ partial melting of a source with a composition similar to the primitive mantle. Thus, the formation of high-chromium, low-calcium garnets with sinusoidal REE patterns could be the first stage of metasomatic enrichment (Pearson et al., 1995; Simon et al., 2007; Agashev et al., 2013; Pokhilenko et al., 2015). The metasomatic agent is strongly HREE depleted and varies significantly in LREE abundances. At this stage, high-chromium garnets are enriched in LREE and the peak shifts from Ce to Nd as the agent/rock ratio is increased (Pokhilenko et al., 2015). The metasomatic agent is rich in incompatible elements, probably of carbonatitic composition.

“Lz 4” garnet formation also occurred during the carbonatite stage of the metasomatic enrichment and is manifested by the near-vertical $\text{CaO-Cr}_2\text{O}_3$ evolution of harzburgitic (“Hz”) to lherzolitic (“Lz 4”) garnet composition. High-chromium garnets are enriched in CaO and LREE and have lherzolitic major-element compositions and harzburgitic REE profiles. The peak concentrations shift to Sm suggesting a high agent/rock ratio. High CaO and LREE concentrations in garnets imply that clinopyroxene formation is not related to this stage of metasomatism (Sobolev et al., 1997a,b, 1999a; Doucet et al., 2013; Howarth et al., 2014).

At the next stage, “Lz 3” and “W” garnets are formed. These garnets are depleted in Cr_2O_3 and enriched in Al_2O_3 , TiO_2 , Y and HREE. They also could inherit high LREE concentrations from “Lz 4” garnets, but their enrichment in HREE testifies for the silicate composition of the metasomatic agent with high LREE. The modeling results show that the composition of the parental melt could be close to the ADP mica-poor picrites. The “Lz 3” garnets are also identified in V. Grib lherzolite samples (Shchukina et al., 2015). “Lz 3” garnets in lherzolite samples are associated but are not in trace element equilibrium with clinopyroxenes (Shchukina et al., 2015). The clinopyroxenes in those lherzolites are in REE equilibrium with a silicate melt that is depleted in LREE and close in composition to the fractionated Turiyno basalt (Shchukina et al., 2015).

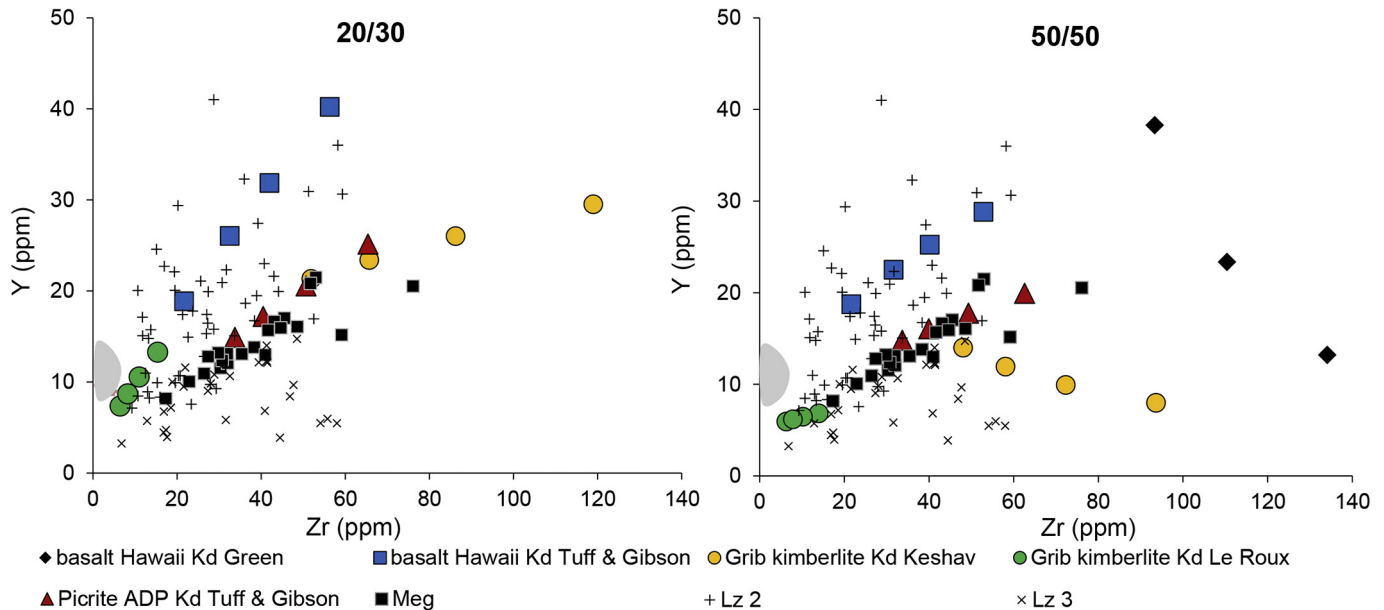


Figure 8. Y-Zr concentrations in V. Grib garnet xenocrysts and in the garnets after fractional crystallization modeling of different types of melts: the Grib kimberlite (“Arkhangelsk.”, 1999), the Hawaii basalt (Hauri, 1996), the ADP alkaline mica-poor picrite (Mahotkin et al., 2000), using mineral/melt partition coefficient from Hauri et al. (1994), Halliday et al. (1995), Green et al. (2000), Le Roex et al. (2003), Keshav et al. (2005), Tuff and Gibson (2007) and different proportions of crystallized minerals (50% grt/50% cpx; 20% grt/30% cpx). Grey field – composition of depleted garnets (“Lz 1”) from V. Grib peridotites (Shchukina et al., 2015).

In the final stage, the garnets are subject to a concurrent decrease in $\text{CaO-Cr}_2\text{O}_3$, depletion of LREE and enrichment in Al_2O_3 , TiO_2 , Y and HREE, and became typical lherzolitic in terms of major and trace element composition, i.e. “Lz 2” garnets. Most probably the metasomatic agent could be of silicate composition with lower LREE concentrations and lower $(\text{La}/\text{Yb})_n$ ratio than the silicate melt in equilibrium with “Lz 3” and “W” garnets. Modeling results show

that the composition of the parental melt is close to OIB. The Y/Zr ratio and modeling results show that the composition of the depleted “Lz 1” garnets also could be regarded as an initial garnet composition for “Lz 2” garnets. Reaction of the basaltic melt with the depleted garnets led to garnet enrichment in LREE, MREE, Y and Zr. Generally, the reaction of silicate melt with peridotites produces enrichment of the rocks in clinopyroxene (Agashev et al., 2013;

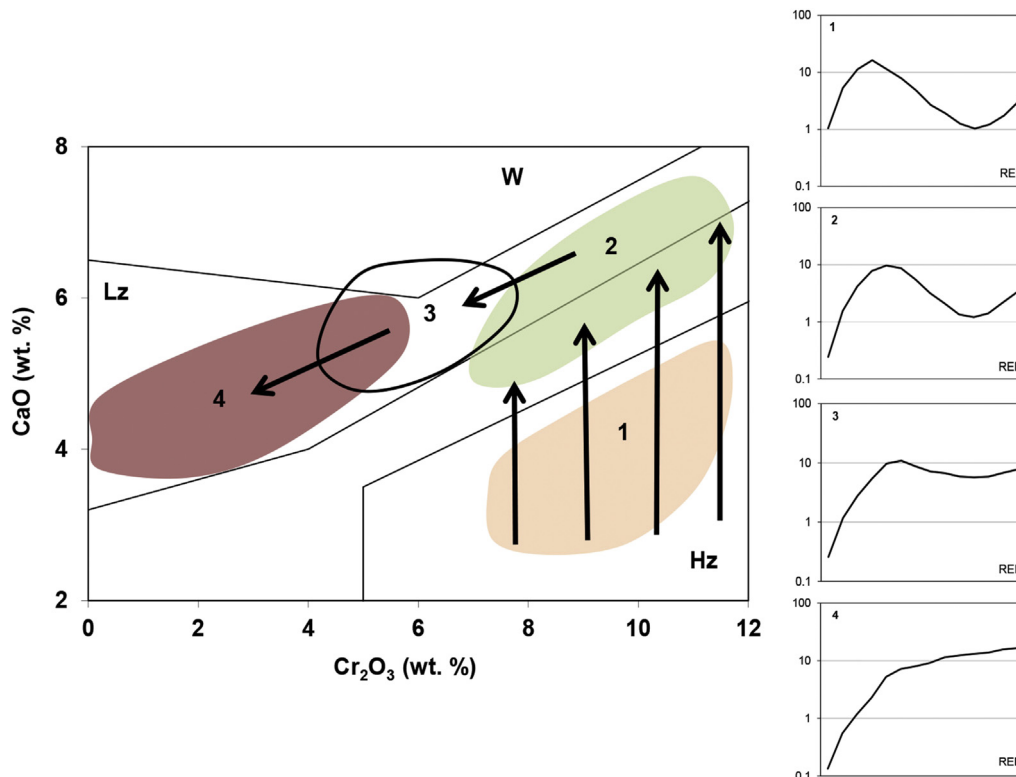


Figure 9. Schematic illustration of the garnet $\text{CaO-Cr}_2\text{O}_3$ evolution.

Howarth et al., 2014; Pokhilenko et al., 2015), e.g. up to 20% of modal clinopyroxene in V. Grib lherzolites (Shchukina et al., 2015). It should be noted that “Lz 2” garnets are in trace element equilibrium with clinopyroxenes in V. Grib lherzolite samples (Shchukina et al., 2015).

Low-chromium megacrysts from kimberlites are commonly interpreted as direct precipitates from magma bodies undergoing normal crystallization fractionation in the deep lithosphere (Nixon and Boyd, 1973a,b; Gurney et al., 1979; Harte and Gurney, 1981; Jones, 1987) in the protokimberlite stage. Based on fractional crystallization calculations (Jones, 1987; Griffin et al., 1997) and isotope data (Griffin et al., 2000; Davies et al., 2001; Nowell et al., 2004) low-Cr megacrysts are supposed to be the product of crystallization of OIB-type asthenospheric magma at high *PT* conditions. The parental (protokimberlitic) magma may evolve to kimberlitic magma as a result of interaction with the lithospheric mantle basement and assimilation of rocks enriched in incompatible elements (Agashev et al., 2006). As modeling results show, V. Grib megacryst formation is not related to kimberlite as previously reported by Kostrovitsky et al. (2004). Partition coefficients are quite variable in the literature, but even within the wide range of available values to choose from Irving and Frey (1978), Fujimaki et al. (1984), Keshav et al. (2005), etc., the parental melt composition yields similar negative results for kimberlite. The excellent correlation between Zr and HREE indicates that the bulk partition coefficient for HREE was less than 1. Zr and HREE behaved as incompatible elements in the melt during garnet crystallization that limits the garnet volume in the crystallizing assemblage to a relatively small proportion (Merry and Le Roex, 2007). Based on REE composition and modeling results, we conclude that “Meg” garnets could be products of direct crystallization of the silicate melt with REE composition close to mica-poor alkaline picrites from ADP. As proposed by Mahotkin et al. (2000), mica-poor alkaline picrites are very similar to those of the “protokimberlite” magmas, calculated to be in equilibrium with sub-calcic clinopyroxene and other megacryst phases in the South Africa group I kimberlites (Jones, 1987; Nowell and Pearson, 1998). These picrites could be minimally lithosphere-contaminated ADP “protokimberlite” magmas.

Based on the present study, the results of two types of mantle metasomatism (silicate and carbonatite), identified by the garnet xenocryst investigation, are graphically demonstrated in Fig. 10. The garnets with $(\text{Sm}/\text{Er})_n > 5$ and low Ti/Eu ratio (“Lz 4”, “Hz”) plot in the field of the carbonatite metasomatism, whereas the garnets

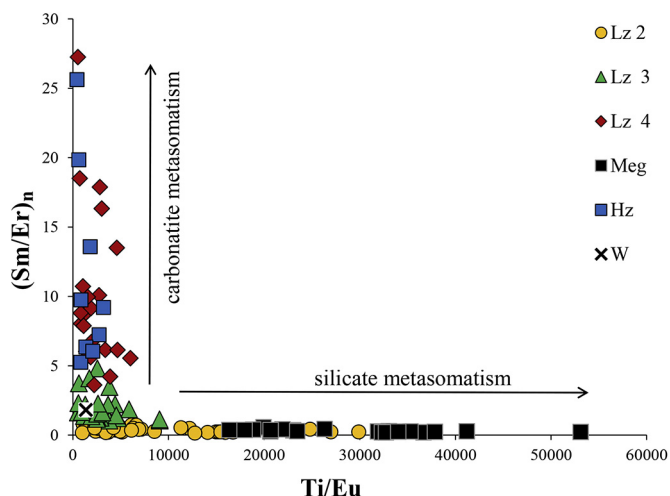


Figure 10. $(\text{Sm}/\text{Er})_n$ vs. Ti/Eu in V. Grib garnet xenocrysts.

with $(\text{Sm}/\text{Er})_n < 1$ (“Lz 2”, “Meg”) lie on the field of the silicate metasomatism. “Lz 3” and “W” garnets have $1 < (\text{Sm}/\text{Er})_n < 5$, matching the transitional position between two metasomatism types. This could be explained by the fact that “Lz 3” and “W” garnets inherited LREE from “Lz 4” garnets and were enriched in HREE under the influence of the silicate melt. *P-T* estimates of the garnet xenocrysts (this work) and peridotites (Shchukina et al., 2015) indicate that the interval of ~60–110 km of the lithospheric mantle beneath the V. Grib pipe was predominantly affected by the silicate melts, whereas the lithospheric mantle deeper than 150 km was influenced by the carbonatite melts. Both types of melts infiltrated into the lithospheric mantle from 110 to 150 km in depth.

7. Conclusions

- (1) The major and trace element composition of garnet xenocrysts from the V. Grib pipe allows us to distinguish three stages of mantle metasomatism under the influence of carbonatite, picrite and basaltic melts. Two types of metasomatic enrichment (carbonatite and silicate) are clearly observed in $(\text{Sm}/\text{Er})_n$ vs. Ti/Eu ratios in the garnet compositions. One garnet grain shows no signs of metasomatic enrichment and its trace element composition is indicative of its residual nature.
- (2) The carbonatite stage of metasomatism resulted in refertilization of the lithospheric mantle, which is demonstrated by the nearly vertical CaO-Cr₂O₃ evolution from harzburgitic to lherzolitic garnet composition. High-chromium harzburgitic garnets with sinusoidal REE patterns could form in the high-degree melt extraction residues also during this stage of metasomatism. At the time of kimberlite eruption, garnets with sinusoidal REE pattern predominantly were located more than 150 km deep in the mantle column.
- (3) Garnets with weakly sinusoidal REE pattern were formed under the influence of the silicate melt with high LREE, probably with REE composition close to the ADP alkaline mica-poor picrites at the next stage of metasomatic events.
- (4) At the last stage of mantle metasomatism, the garnets show a concurrent decrease in CaO-Cr₂O₃ and became typical lherzolitic with flat REE patterns under the influence of the basaltic melts. Abundance of the lherzolitic garnets with flat REE patterns and *P-T* estimates evidenced to extensive percolation of basaltic melts through all sections of the lithospheric mantle to a depth of 160 km.
- (5) Formation of Cr-poor garnets of megacryst paragenesis with flat REE pattern is not related to host kimberlite. These garnets could be the product of direct crystallization of the silicate melt with REE composition close to the ADP alkaline mica-poor picrites.

Acknowledgements

The work was supported by the FBRF (Grants No. 15-05-07758) and by state assignment project No. VIII.72.1.1. We are thankful to N.V. Sobolev and anonymous reviewer for constructive reviews that resulted in significant improvement of the manuscript. We are grateful to N.N. Golovin, the chief geologist of the Arkhangelsk-geoldobycha Joint-Stock Company, for providing samples. We also thank to I.V. Ashchepkov, I.Yu. Safonova and Nick Roberts for constructive discussion.

Appendix A. Supplementary data

Supplementary data related to this article can be found at <http://dx.doi.org/10.1016/j.gsf.2016.08.005>.

References

- Achterbergh, E.V., Griffin, W., Stiefenhofer, J., 2001. Metasomatism in mantle xenoliths from the Lethakane kimberlites: estimation of element fluxes. *Contributions to Mineralogy and Petrology* 141, 397–414.
- Afanasyev, V.P., Ashchepkov, I.V., Verzhak, V.V., O'Brien, H.O., Palessky, S.V., 2013. PT conditions and trace element variations of picroilmenites and pyropes from placers and kimberlites in the Arkhangelsk region, NW Russia. *Journal of Asian Earth Sciences* 70–71, 45–63.
- Agashev, A.M., Watanabe, T., Budaev, D.A., Pokhilenko, N.P., Fomin, A.S., Maehara, K., Maeda, J., 2001. Geochemistry of kimberlites from Nakyn field, Siberia: evidence for unique source composition. *Geology* 29 (3), 267–270.
- Agashev, A.M., Pokhilenko, N.P., Malkovets, V.G., Sobolev, N.V., 2006. Sm–Nd isotopic system in garnet megacrysts from the Udachnaya kimberlite pipe (Yakutia) and petrogenesis of kimberlites. *Earth Sciences Reports* 407A (3), 491–494.
- Agashev, A.M., Pokhilenko, N.P., Takazawa, E., McDonald, J.A., Vavilov, M.A., Watanabe, T., Sobolev, N.V., 2008. Primary melting sequence of a deep (>250 km) lithospheric mantle as recorded in the geochemistry of kimberlite–carbonatite assemblages, Snap Lake dyke system, Canada. *Chemical Geology* 255 (3–4), 317–328.
- Agashev, A.M., Ionov, D.A., Pokhilenko, N.P., Golovin, A.V., Cherepanova, Yu, Sharygin, I.S., 2013. Metasomatism in the lithospheric mantle roots: constraints from WR and minerals chemical composition of deformed peridotite xenoliths from the Udachnaya kimberlite pipe. *Lithos* 160–161, 201–215.
- Ashchepkov, I.V., Pokhilenko, N.P., Vladykin, N.V., Logvinova, A.M., Kostrovitsky, S.I., Afanasyev, V.P., Pokhilenko, L.N., Kuligin, S.S., Malygina, L.V., Alymova, N.V., Khmelnikova, O.S., Palessky, S.V., Nikolaeva, I.V., Karpenko, M.A., Stagnitsky, Y.B., 2010. Structure and evolution of the lithospheric mantle beneath Siberian craton, thermobarometric study. *Tectonophysics* 485, 17–41.
- Ashchepkov, I.V., Andre, L., Downes, H., Belyatsky, B.A., 2011. Pyroxenites and megacrysts from Vitim picrite–basalts (Russia): polybaric fractionation of rising melts in the mantle? *Journal of Asian Earth Sciences* 42, 14–37.
- Ashchepkov, I.V., Rotman, A.Y., Somov, S.V., Afanasyev, V.P., Downes, H., Logvinova, A.M., Nossyko, S., Shimupi, J., Palessky, S.V., Khmelnikova, O.S., Vladykin, N.V., 2012. Composition and thermal structure of the lithospheric mantle beneath kimberlite pipes from the Catoca cluster, Angola. *Tectonophysics* 530–531, 128–151.
- Bell, D.R., Gregoire, M., Grove, T.L., Chatterjee, N., Carlson, R.W., Buseck, P.R., 2005. Silica and volatile-element metasomatism of Archean mantle: a xenoliths-scale example from the Kaapvaal Craton. *Contributions to Mineralogy and Petrology* 150, 251–267.
- Bogatikov, O.A., Garanin, V.K., Kononova, V.A., Kudryavceva, G.P., Vasil'eva, E.R., Verzhak, V.V., Verichev, E.M., Parsadanyan, K.S., Posuhova, T.V., 1999. Arkhangelsk Diamondiferous Province. Moscow State University, p. 521 (in Russian).
- Boyd, F.R., Pokhilenko, N.P., Pearson, D.G., Mertzman, S.A., Sobolev, N.V., Finger, L.W., 1997. Composition of the Siberian cratonic mantle: evidence from Udachnaya peridotite xenoliths. *Contributions to Mineralogy and Petrology* 128 (2–3), 228–246.
- Brey, G.P., Kohler, T., 1990. Geothermobarometry in four-phase lherzolites. II. New thermobarometers, and practical assessment of existing thermobarometers. *Journal of Petrology* 31, 1353–1378.
- Burgess, S.R., Harte, B., 2004. Tracing lithosphere evolution through the analyses of heterogeneous G9/G10 garnet in peridotite xenoliths, II: REE chemistry. *Journal of Petrology* 45 (3), 609–634.
- Canil, D., Wei, K., 1992. Constraints on the origin of mantle-derived low Ca garnets. *Contributions to Mineralogy and Petrology* 109, 421–430.
- Carswell, D.A., 1973. Primary and secondary phlogopites and clinopyroxenes in garnet lherzolite xenoliths. In: Ahrean, L.H., Duncan, A.R., Erlank, A.J. (Eds.), *International Conference on Kimberlites (Extended Abstracts)*, Cape Town, South Africa. Pergamon Press, Oxford.
- Coltorti, M., Bonadiman, C., Hinton, R.W., Siena, F., Upton, B.G.J., 1999. Carbonatite metasomatism of the oceanic upper mantle: evidence from clinopyroxene and glasses in ultramafic xenoliths of Grande Comore, Indian Ocean. *Journal of Petrology* 40, 133–165.
- Davies, G.R., Spriggs, A.J., Nixon, P.H., 2001. A non-cognate origin for the Gibeon kimberlite megacryst suite, Namibia: implications for the origin of Namibian kimberlites. *Journal of Petrology* 42, 159–172.
- Dawson, J.B., 2004. A fertile harzburgite–garnet lherzolite transition: possible inferences for the roles of strain and metasomatism in upper mantle peridotites. *Lithos* 77, 553–569.
- Dawson, J.B., Stephens, W.E., 1975. Statistical analysis of garnets from kimberlites and associated xenoliths. *Journal of Geology* 83, 589–607.
- Doucet, L.S., Ionov, D.A., Golovin, A.V., 2013. The origin of coarse garnet peridotites in cratonic lithosphere: new data on xenoliths from the Udachnaya kimberlite, central Siberia. *Contributions to Mineralogy and Petrology* 165, 1225–1242.
- Efimova, E.S., Sobolev, N.V., 1977. Abundance of crystalline inclusions in Yakutian diamonds. *Doklady Akademii Nauk SSSR* 237, 1475–1478 (in Russian).
- Erlank, A.J., Waters, F.G., Hawkesworth, C.J., Haggerty, S.E., Allsopp, H.L., Rickard, R.S., Menzies, M., 1987. Evidence for mantle metasomatism in peridotite nodules from the Kimberly pipes, South Africa. In: Menzies, M., Hawkesworth, C.J. (Eds.), *Mantle Metasomatism*. Academic Press, London, pp. 221–235.
- Fujimaki, H., Tatsumoto, M., Aoki, K.-I., 1984. Partition coefficients of Hf, Zr, and REE between phenocrysts and groundmasses. *Journal of Geophysical Research* 89, 662–672.
- Garanin, V.K., 2004. *Alkaline Ultrabasic Rocks in the Arkhangelsk Diamondiferous Province: Present State of Knowledge and Prospects for Studies*, vol. 59(1). Moscow University Geology Bulletin, pp. 35–45.
- Gibson, S.A., Malarkey, J., Day, A.A., 2008. Melt depletion and enrichment beneath the western Kaapvaal Craton: evidence from Finsch peridotite xenoliths. *Journal of Petrology* 49, 1817–1852.
- Green, T., Blundy, J., Adam, J., Yaxley, G., 2000. SIMS determination of trace element partition coefficients between garnet, clinopyroxene and hydrous basaltic liquids at 2–7.5 GPa and 1080–1200 °C. *Lithos* 53, 165–187.
- Gregoire, M., Bell, D.R., Le Roex, A.P., 2003. Garnet lherzolites from the Kaapvaal craton (South Africa): trace element evidence for a metasomatic history. *Journal of Petrology* 44 (4), 629–657.
- Griffin, W.L., Moore, R.O., Ryan, C.G., Gurney, J.J., Win, T.T., 1997. Geochemistry of magnesian ilmenite megacrysts from Southern African kimberlites. *Russian Geology and Geophysics* 38, 421–443.
- Griffin, W.L., Shee, S.R., Ryan, C.G., Win, T.T., Wyatt, B.A., 1999. Harzburgite to lherzolite and back again: metasomatic processes in ultramafic xenoliths from the Wesselton kimberlite, Kimberly, South Africa. *Contributions to Mineralogy and Petrology* 134, 232–250.
- Griffin, W.L., Pearson, N.J., Belousova, E.A., Jackson, S.E., O'Reilly, S.Y., van Achterbergh, E., Shee, S.R., 2000. The Hf isotope composition of cratonic mantle: LAM-MC-ICPMS analysis of zircon megacrysts in kimberlites. *Geochimica et Cosmochimica Acta* 64, 133–147.
- Griffin, W.L., O'Reilly, S.Y., Abe, N., Aulbach, S., Davies, R.M., Pearson, N.J., Doyle, B.J., Kivi, K., 2003. The origin and evolution of Archean lithospheric mantle. *Pre-Cambrian Research* 27, 19–41.
- Gurney, J.J., 1984. A correlation between garnets and diamonds. In: Glover, J.E., Harris, P.G. (Eds.), *Kimberlite Occurrence and Origin: A Basis for Conceptual Models in Exploration*, vol. 8. Geol. Dept. and Univ. Ext., Univ. of WA, Publ., pp. 143–166.
- Gurney, J.J., Jacob, W.R.O., Dawson, J.B., 1979. Megacrysts from the monastery pipe, South Africa. In: Boyd, F.R., Meyer, H.O.A. (Eds.), *Proceedings of the 2-nd International Kimberlite Conference*, vol. 2. American Geophysical Union, pp. 227–243.
- Halliday, A.N., Lee, D.C., Tommasini, S., Davies, G.R., Paslick, C.R., Fitton, J.G., James, D.E., 1995. Incompatible trace-elements in OIB and MORB and source enrichment in the sub-oceanic mantle. *Earth and Planetary Science Letters* 133 (3–4), 379–395.
- Harte, B., 1983. Mantle peridotites and processes – the kimberlite sample. In: Hawkesworth, C.J., Norry, M.J. (Eds.), *Continental Basalts and Mantle Xenoliths*, pp. 6–91.
- Harte, B., Gurney, J.J., 1981. The model of formation of the Cr-poor megacryst suite from kimberlites. *Journal of Geology* 89, 749–753.
- Hauri, E.H., 1996. Major-element variability in the Hawaiian mantle plume. *Nature* 382, 415–419.
- Hauri, E.H., Wagner, T.P., Grove, T.L., 1994. Experimental and natural partitioning of Th, U, Pb and other trace elements between garnet, clinopyroxene and basaltic melts. *Chemical Geology* 117, 149–166. [http://dx.doi.org/10.1016/0009-2541\(94\)90126-0](http://dx.doi.org/10.1016/0009-2541(94)90126-0).
- Hoal, K.E.O., Hoal, B.G., Erlank, A.J., Shimizu, N., 1994. Metasomatism of the mantle lithosphere recorded by rare earth elements in garnets. *Earth and Planetary Science Letters* 126, 303–313.
- Howarth, G.H., Barry, P.H., Pernet-Fisher, J.F., Baziotis, I.P., Pokhilenko, N.P., Pokhilenko, L.N., Bodnar, R.J., Taylor, L.A., Agashev, A.M., 2014. Superplume metasomatism: evidence from Siberian mantle xenoliths. *Lithos* 184–187, 209–224.
- Irving, A.J., Frey, F.A., 1978. Distribution of trace-elements between garnet megacrysts and host volcanic liquids of kimberlitic to rhyolitic composition. *Geochimica et Cosmochimica Acta* 42 (NA6), 771–787.
- Jones, R.A., 1987. Strontium and neodymium isotope and rare earth element evidence for the genesis of megacrysts in kimberlites of southern Africa. In: Nixon, P.H. (Ed.), *Mantle Xenoliths*. John Wiley and Son, New York, U.S.A., pp. 711–724.
- Kamenetsky, V.S., Yaxley, G.M., 2015. Carbonate–silicate liquid immiscibility in the mantle propels kimberlite magma ascent. *Geochimica et Cosmochimica Acta* 158, 48–56.
- Kamenetsky, V.S., Kamenetsky, M.B., Weiss, Y., Navon, O., Nielsen, T.F.D., Mernagh, T.P., 2009. How unique is the Udachnaya-East kimberlite? Comparison with kimberlites from the Slave Craton (Canada) and SW Greenland. *Lithos* 112, 334–346.
- Keshav, S., Corgne, A., Gudfinnsson, G.H., Bizmis, M., McDonough, W.F., Fei, Y., 2005. Kimberlite petrogenesis: insight from clinopyroxene–melt partitioning experiments at 6 GPa in the CaO–MgO–Al₂O₃–SiO₂–CO₂ system. *Geochimica et Cosmochimica Acta* 69 (11), 2829–2845.
- Kostrovitsky, S.I., Malkovets, V.G., Verichev, E.M., Garanin, V.K., Suvorova, L.V., 2004. Megacrysts from the V. Grib kimberlite pipe. *Lithos* 77, 511–523.
- Lavrent'ev, Y.G., Korolyuk, V.N., Usova, L.V., Logvinova, A.M., 2006. Electron probe microanalysis of pyropes for nickel traces as applied to study of the geothermometry of peridotites. *Russian Geology and Geophysics (Geologiya i Geofizika)* 47 (10), 1086–1089 (1075–1078).

- Lavrent'ev, Y.G., Korolyuk, V.N., Usova, L.V., Nigmatulina, E.N., 2015. Electron probe microanalysis of rock-forming minerals with a JXA-8100 electron probe microanalyzer. *Russian Geology and Geophysics* 56, 1428–1436.
- Lehtonen, M., O'Brien, H., Peltonen, P., Kukkonen, I., Ustinov, V., Verzhak, V., 2009. Mantle xenocrysts from the Arkhangelskaya kimberlite (Lomonosov mine, NW Russia): constraints on the composition and thermal state of the diamondiferous lithospheric mantle. *Lithos* 112 (2), 924–933.
- MacGregor, J.D., 1964. The Reaction: 4 Enstatite + Spinel = Forsterite + Pyrope, vol. 63. Carnegie Inst. Wash. Yb., pp. 157–160.
- MacGregor, I., 1974. The system MgO–Al₂O₃–SiO₂: solubility of Al₂O₃ in enstatite for spinel and garnet peridotite composition. *American Mineralogy* 59, 110–119.
- Mahotkin, I.L., Gibson, S.A., Thompson, R.N., Zhuravlev, D.Z., Zherdev, P.U., 2000. Late Devonian diamondiferous kimberlite and alkaline picrite (proto-kimberlite?) magmatism in the Arkhangelsk region, Russia. *Journal of Petrology* 41 (2), 201–227.
- Malkovets, V.G., Zedgenizov, D.A., Sobolev, N.V., Kuzmin, D.V., Gibsher, A.A., Shchukina, E.V., Golovin, N.N., Verichev, E.M., Pokhilenko, N.P., 2011. Contents of trace elements in olivines from diamonds and peridotite xenoliths of the V. Grib kimberlite pipe (Arkhangelsk diamondiferous province, Russia). *Doklady Earth Sciences* 436 (2), 219–223.
- McDonough, W.S., Sun, S.S., 1995. The composition of the Earth. *Chemical Geology* 120, 223–253.
- Menzies, M.A., Hawkesworth, C.J., 1987. *Mantle Metasomatism*. Academic Press, London, Orlando, p. 472.
- Menzies, M.A., Rogers, N., Tindle, A., Hawkesworth, C.J., 1987. Metasomatic and enrichment processes in lithospheric peridotites, an effect of asthenosphere–lithosphere interaction. In: Menzies, M.A., Hawkesworth, C.J. (Eds.), *Mantle Metasomatism*. Academic Press Inc., London, UK, pp. 313–361.
- Merry, M., Le Roex, A., 2007. Megacryst suites from the Lekkerfontein and Uintjiesberg kimberlites, southern Africa: evidence for a non-cognate origin. *Southern African Journal of Geology* 110, 597–610.
- Nickel, K.G., Green, D.H., 1985. Empirical geothermobarometry for garnet peridotites and implications for the nature of the lithosphere kimberlites and diamonds. *Earth and Planetary Science Letters* 73, 158–170.
- Nixon, P.H., Boyd, E.R., 1973a. The discrete nodule (megacryst) association in kimberlites from northern Lesotho. In: Nixon, P.H. (Ed.), *Lesotho Kimberlites*. Cape and Transvaal Printers, South Africa, pp. 67–75.
- Nixon, P.H., Boyd, E.R., 1973b. Petrogenesis of the granular and sheared ultrabasic nodule suite in kimberlite. In: Nixon, P.H. (Ed.), *Lesotho Kimberlites*. Cape and Transvaal Printers, South Africa, pp. 48–56.
- Nowell, G.M., Pearson, D.G., 1998. Hf isotope constraints on the genesis of kimberlitic megacrysts: evidence for a deep-mantle component in kimberlites. In: *Extended Abstracts: 7-th International Kimberlite Conference*. University of Cape Town, Cape Town, pp. 634–636.
- Nowell, G.M., Pearson, D.G., Bell, D.R., Carlson, R.W., Smith, C.B., Kempton, P.D., Noble, S.R., 2004. Hf isotope systematics of kimberlites and their megacrysts: new constraints on their source regions. *Journal of Petrology* 45, 1583–1612.
- Pearson, D.G., Shirey, S.B., Carlson, R.W., Boyd, F.R., Pokhilenko, N.P., Shimizu, N., 1995. Re-Os, Sm-Nd, and Rb-Sr isotope evidence for thick Archaean lithospheric mantle beneath the Siberian craton modified by multistage metasomatism. *Geochimica et Cosmochimica Acta* 59, 959–977.
- Pokhilenko, N.P., Sobolev, N.V., Boyd, F.R., Pearson, D.G., Shimizu, N., 1993. Megacrystalline pyrope peridotites in the lithosphere of the Siberian platform: mineralogy, geochemical peculiarities and the problem of their origin. *Russian Geology and Geophysics* 34, 56–67 (in Russian).
- Pokhilenko, N., Sobolev, N.V., Kuligin, S.S., Shimizu, N., 1999. Peculiarities of distribution of pyroxenite paragenesis garnets in Yakutian kimberlite and some aspects of the evolution of the Siberian Craton lithospheric mantle. In: *Proceedings of the 7th International Kimberlite Conference*, vol. 2, pp. 689–698.
- Pokhilenko, N.P., Agashev, A.M., Litasov, K.D., Pokhilenko, L.N., 2015. Carbonatite metasomatism of peridotite lithospheric mantle: implications for diamond formation and carbonatite-kimberlite magmatism. *Russian Geology and Geophysics* 56 (1–2), 280–295.
- Pollack, H.N., Chapman, D.S., 1977. On the regional variation of heat flow geotherms and lithospheric thickness. *Tectonophysics* 38, 279–296.
- Le Roex, A.P., Bell, D.R., Davis, P., 2003. Petrogenesis of group 1 kimberlites from Kimberley, South Africa: evidence from bulk-rock geochemistry. *Journal of Petrology* 44 (12), 2261–2286.
- Ryan, C.G., Griffin, W.L., Pearson, N.J., 1996. Garnet geotherms: a technique for derivation of P–T data from Cr-pyrope garnets. *Journal of Geophysical Research* 101, 5611–5625.
- Sablukov, S.M., Sablukova, L.I., Shavyrina, M.V., 2000. Mantle xenoliths from the Zimmii Bereg kimberlite deposits of rounded diamonds, Arkhangelsk diamondiferous province. *Petrologia* 8 (5), 518–548 (in Russian).
- Shchukina, E.V., Golovin, N.N., Malkovets, V.G., Pokhilenko, N.P., 2012. Mineralogy and equilibrium P–T estimates for peridotite assemblages from the V. Grib kimberlite pipe (Arkhangelsk kimberlite province). *Doklady Earth Science* 444 (2), 776–781.
- Shchukina, E.V., Agashev, A.M., Golovin, N.N., Pokhilenko, N.P., 2013. Evidence of Mantle Metasomatism in Garnet Peridotites from the V. Grib Kimberlite Pipe (Arkhangelsk Region, Russia). EGU General Assembly, ID. EGU2013–9456.
- Shchukina, E.V., Agashev, A.M., Kostrovitsky, S.I., Pokhilenko, N.P., 2015. Metasomatic events in the lithospheric mantle beneath the V. Grib kimberlite pipe (Arkhangelsk diamondiferous province). *Russian Geology and Geophysics* 56 (12), 1701–1716.
- Shevchenko, S.S., Lokhov, K.I., Sergeev, S.A., 2004. Isotope studies in VSEGEI. Prospects of application of results for predicting and search of diamond deposits. In: *Proceedings of Scientific Practical Conference on Efficiency of Prediction and Search for Diamond Deposits: Past, Present, and Future*, St. Petersburg, pp. 383–387.
- Shimizu, N., Richardson, S.H., 1987. Trace element abundance patterns of garnet inclusions in peridotite suite diamonds. *Geochimica et Cosmochimica Acta* 51, 755–758.
- Shimizu, N., Pokhilenko, N.P., Boyd, F.R., Pearson, D.G., 1997a. Geochemical characteristics of mantle xenoliths from the Udachnaya kimberlite pipe. *Russian Geology and Geophysics* 38, 205–217.
- Shimizu, N., Sobolev, N.V., Yefimova, E.S., 1997b. Chemical heterogeneity of garnet inclusions and juvenility of peridotite diamonds from Siberia. *Russian Geology and Geophysics* 38, 356–372.
- Shu, Q., Brey, G.P., 2015. Ancient mantle metasomatism recorded in subcalcic garnet xenocrysts: temporal links between mantle metasomatism, diamond growth and crustal tectonomagmatism. *Earth and Planetary Science Letters* 418, 27–39.
- Simon, N.S.C., Irving, G.J., Davies, G.R., Pearson, D.G., Carlson, R.W., 2003. The origin of garnet and clinopyroxene in “depleted” Kaapvaal peridotites. *Lithos* 71, 289–322.
- Simon, N.S.C., Carlson, R.W., Pearson, D.G., Davies, G.R., 2007. The origin and evolution of the Kaapvaal cratonic lithospheric mantle. *Journal of Petrology* 48, 589–625.
- Sobolev, N.V., 1977. Deep-Seated Inclusions in Kimberlites and the Problem of the Composition of the Upper Mantle. American Geophysical Union, Washington, D.C.
- Sobolev, N.V., Lavrentiev, Y.G., Pospelova, L.N., Sobolev, E.V., 1969. Chrome pyropes from Yakutian diamonds. *Doklady Akademii Nauk SSSR* 189 (1), 162–165.
- Sobolev, N.V., Lavrentyev, Y.G., Pokhilenko, N.P., Usova, L.V., 1973. Chrome-rich garnets from the kimberlites of Yakutia and their parageneses. *Contributions to Mineralogy and Petrology* 40, 39–52.
- Sobolev, N.V., Pokhilenko, N.P., Grib, V.P., Skripnichenko, V.A., Titova, V.E., 1992. Peculiarities of composition and origin conditions of deep seated minerals in diatremes from Omega peninsula and kimberlites from Zimny Bereg of the Arkhangelsk province. *Russian Geology and Geophysics* 10, 84–93.
- Sobolev, V.N., Taylor, L.A., Snyder, G.A., Sobolev, N.V., Pokhilenko, N.P., Kharkiv, A.D., 1997a. A unique metasomatized peridotite xenolith from the Mir kimberlite, Siberian platform. *Russian Geology and Geophysics* 38, 218–228.
- Sobolev, N.V., Yefimova, E.S., Reimers, L.F., Zakharchenko, O.D., Makhin, A.I., Usova, L.V., 1997b. Mineral inclusions in the diamonds of Arkhangelsk kimberlite province. *Geologiya i Geofizika* 38 (2), 358–370.
- Sobolev, V.N., Taylor, L.A., Snyder, G.A., Jerde, E.A., Neal, C.R., Sobolev, N.V., 1999a. Quantifying the effects of metasomatism of mantle xenoliths: constraints from secondary chemistry and mineralogy in Udachnaya eclogites, Yakutia. *International Geology Review* 41, 391–416.
- Sobolev, N.V., Sobolev, V.N., Snyder, G.A., Yefimova, E.S., Taylor, L.A., 1999b. Significance of eclogitic and related paragenesis of natural diamonds. *International Geology Review* 41, 129–140.
- Sobolev, N.V., Logvinova, A.M., Efimova, E.S., 2009a. Syngenetic phlogopite inclusions in kimberlite hosted diamonds: implications for role of volatiles in diamond formation. *Russian Geology and Geophysics* 50 (12), 1234–1248.
- Sobolev, N.V., Logvinova, A.M., Zedgenizov, D.A., Pokhilenko, N.P., Malygina, E.V., Kuzmin, D.V., Sobolev, A.V., 2009b. Petrogenetic significance of minor elements in olivines from diamonds and peridotite xenoliths of Yakutia. *Lithos* 112, 701–713.
- Solovyeva, L.V., Yasnygina, T.A., Egorov, K.N., 2012. Metasomatic parageneses in deep-seated xenoliths from Udachnaya and Komsomolskaya-Magnitnaya pipes as indicators of fluid transfer through the mantle lithosphere of the Siberian craton. *Russian Geology and Geophysics* 53, 1304–1323.
- Stachel, T., Viljoen, K.S., Brey, G., Harris, J.W., 1998. Metasomatic processes in Iherzolitic and harzburgitic domains of diamondiferous lithospheric mantle. *Earth and Planetary Science Letters* 159, 1–12.
- Stachel, T., Aulbach, S., Brey, G.P., Harris, J.W., Leost, I., Tapper, R., Viljoen, K.S., 2004. The trace element composition of silicate inclusions in diamonds: a review. *Lithos* 77, 1–19.
- Taylor, W.R., 1998. An experimental test of some geothermometer and geobarometer formulations for upper mantle peridotites with application to the thermobarometry of fertile Iherzolite and garnet websterite. *Neues Jahrbuch für Mineralogie Abhandlungen* 172, 381–408.
- Tuff, J., Gibson, S., 2007. Trace-element partitioning between garnet, clinopyroxene and Fe-rich picritic melts at 3 to 7 Gpa. *Contributions to Mineralogy and Petrology* 153, 369–387.
- Tychkov, N.S., Agashev, A.M., Malygina, E.V., Nikolenko, E.I., Pokhilenko, N.P., 2014. Thermal perturbations in the lithospheric mantle as evidenced from P–T equilibrium conditions of xenoliths from the Udachnaya kimberlite pipe. *Doklady Earth Science* 454 (1), 84–88.
- Ziberna, L., Nimis, P., Zanetti, A., Marzoli, A., Sobolev, N., 2013. Metasomatic processes in the central Siberian cratonic mantle: evidence from garnet xenocrysts from the Zagadochnaya kimberlite. *Journal of Petrology* 54 (11), 2379–2409.